tvst

Uveitis

Evaluation of the Dose-Dependent Inflammatory Response and No-Observable Adverse Effect Level of Intravitreal Endotoxin in the African Green Monkey

Tatiana M. Corey[1], Vernard V. Woodley[1], Merissa O'Connor[1], Emma Connolly[2,3], Sarah Doyle[2,3], Stephanie Shrader[4], Cyrene Phipps[1], Kimicia Isaac[1], and Matthew Lawrence[1]

[1] Virscio, Inc., New Haven, CT, USA
[2] Trinity College Institute of Neuroscience, Trinity College Dublin, Dublin, Ireland
[3] Department of Clinical Medicine, School of Medicine, Trinity College Dublin, Dublin, Ireland
[4] StageBio, Mount Jackson, VA, USA

Correspondence: Tatiana M. Corey, Virscio, Inc., 4 Science Park, New Haven, CT 06511, USA.
e-mail: corey@uthscsa.edu

Received: April 12, 2022
Accepted: July 18, 2022
Published: August 18, 2022

Keywords: endotoxin; uveitis; toxicity; animal model; intravitreal

Citation: Corey TM, Woodley VV, O'Connor M, Connolly E, Doyle S, Shrader S, Phipps C, Isaac K, Lawrence M. Evaluation of the dose-dependent inflammatory response and no-observable adverse effect level of intravitreal endotoxin in the African green monkey. Transl Vis Sci Technol. 2022;11(8):17, https://doi.org/10.1167/tvst.11.8.17

Purpose: To evaluate the inflammatory effects and no-observed adverse effect level (NOAEL) of intravitreal endotoxin in an African green monkey model of uveitis.

Methods: Fifteen green monkeys were administered intravitreal endotoxin ranging from 0.005 to 0.08 endotoxin unit (EU)/eye. Inflammation was evaluated by slit-lamp biomicroscopy, indirect fundoscopy, tonometry, color fundus photography, ocular coherence tomography, laser flare photometry, and histopathology, with analysis of cytokine levels in aqueous and vitreous humor. The inter-rater reliability of a refined nonhuman primate ophthalmic scoring system was evaluated.

Results: A dose-dependent inflammatory response was observed beginning at 0.02 EU/eye; no inflammatory response exceeding the vehicle was observed at 0.005 EU/eye. Retinal pathology was minimal, and posterior visualization degraded with increasing inflammation. Inflammation was observed by histopathology at 0.04 EU/eye. Inter-rater reliability of the scoring system was high, with 99.2% of individual scores differing by 1 scale unit or less and 87.2% of summary scores differing by 2 scale units or less.

Conclusions: The NOAEL for intravitreal endotoxin in the green monkey is 0.005 EU/eye, with inflammation increasing with increasing dose beginning at 0.02 EU/eye. This updated nonhuman primate ophthalmic scoring system allows for high inter-rater reliability for the quantification of mild to severe inflammation in the green monkey eye.

Translational Relevance: Validation of the ophthalmic inflammation scoring system enables application of the green monkey as a valuable translational model. Candidate therapeutics should be confirmed to have endotoxin levels below this threshold before safety testing in this species to enable interpretation of inflammation and minimize impact on animal welfare.

Introduction

Endotoxin is a lipopolysaccharide cell wall antigen found in the outer membrane of Gram-negative bacteria. As a potent activator of the inflammatory process, the presence of endotoxin can trigger a severe inflammatory response both by acting as a pyrogen and by triggering proinflammatory cytokine release by immunocytes.[1] Concentrations that trigger inflammatory effects are dependent on the route, frequency and duration of administration, and species susceptibility.[2]

Endotoxin contamination presents a significant risk to the use of pharmaceutical products and biomedical devices. Ubiquitous in nature, endotoxin is often introduced during compound or device manufacturing; endotoxin is stable under extreme conditions and is therefore challenging and expensive to completely

eliminate from the manufacturing process.[1] To achieve a clear understanding of the safety of pharmacological compounds for each route of administration or target tissue compartment, it is critical to define the no-observed adverse effect level (NOAEL) of endotoxin. For safety testing in animal models, candidate therapeutic compounds should be evaluated to confirm endotoxin levels below the NOAEL threshold to avoid confounding the interpretation of detected inflammation and minimize impact on animal welfare.

Current understanding of the NOAEL of intraocular endotoxin in animal models is limited. Three reported studies have evaluated the effect of intravitreal endotoxin, quantified in endotoxin units (EU), in animal model species, including two in rabbits and a single study in cynomolgus macaques.[3,4,5] In rabbits, a NOAEL was identified as 0.01 EU/eye following evaluation of the dose range from 0.01 to 0.75 EU/eye. Dose-related inflammation was identified beginning at 0.05 EU/eye, with histopathological changes identified at 0.1 EU/eye.[4] Similar response was observed in the cynomolgus macaque with the scoring system and instrumentation applied, with a NOAEL of 0.01 EU/eye when evaluating a dose range from 0.01 to 0.51 EU/eye. Dose-related inflammation was identified in the cynomolgus monkeys beginning at 0.04 EU/eye, and histopathological changes were seen at 0.21 EU/eye.[5] These studies provide valuable comparative biology references for evaluation of the NOAEL in other preclinical species and humans.

The green monkey is an Old World monkey inhabiting sub-Saharan Africa. It was introduced as an invasive species in the West Indian islands of St. Kitts, Nevis, and Barbados, and today the green monkey has an estimated St. Kitts population exceeding 30,000.[6,7] The isolated island biogeography has prevented exposure to common nonhuman primate zoonoses, and green monkeys are not carriers of the fatal *Macacine herpesvirus 1* (B virus), a substantial occupational health risk associated with working with macaque species.[6,7] These qualities have made the green monkey, and particularly those of the St. Kitts population, a valuable resource for biomedical study, with increasing application to the elucidation of ocular pathophysiology, as well as therapeutic safety and efficacy.[8–14]

The purpose of this study was to evaluate the dose-related inflammatory response and NOAEL following intravitreal administration of endotoxin in an African green monkey model of uveitis. Evaluation of ocular inflammation in this modal allows us to test the hypothesis that the green monkey exhibits a sensitivity to intravitreal endotoxin similar to that of the cynomolgus macaque and rabbit. An additional objective was to characterize the degradation of image quality with progressive inflammation and to establish the inter-rater reliability of a nonhuman primate ophthalmic examination scoring system, derived from the Hackett–McDonald scoring system and Nussenblatt Scale for vitreous haze, tailored specifically to the African green monkey.[15–20]

Materials and Methods

Subjects

The study was conducted in a Virscio examination and procedure room located at the St. Kitts Biomedical Research Foundation (St. Kitts, West Indies). A total of 15 (five male, 5.8–7.1 kg; 10 female, 3.3–5.3 kg) adult African green monkeys (*Chlorocebus sabaeus*) were enrolled and evaluated in the study in accordance with the ARVO Statement for the Use of Animals in Ophthalmic and Vision Research and a protocol approved by the facility Institutional Animal Care and Use Committee. Prescreen veterinary physical examinations were performed to confirm general health. Prescreen ophthalmic examinations to confirm ophthalmic health and collect baseline data included tonometry, slit-lamp biomicroscopy, fundoscopy, color fundus photography (CFP), laser flare photometry, and anterior segment and posterior segment optical coherence tomography (OCT). Animals were sedated by intramuscular (IM) injection of a ketamine and xylazine cocktail (8 mg/kg and 1.6 mg/kg, respectively) to effect for examination and treatment procedures. Fifteen monkeys with normal findings were enrolled in the study and randomized into five treatment groups (Table 1). Monkeys were maintained in paired or single housing for the duration of the study. General wellbeing was confirmed twice daily by cage-side observations beginning 1 week prior to dosing. Daily individual food consumption was assessed by visual inspection of the feed pan or cage floor prior to cage washing following routine feeding for overall appetite. All monkeys were offered supplemental fruit on every day requiring sedation. Body weights were monitored throughout the study.

Test Article

The test article was commercially sourced 10,000-EU United States Pharmacopeia reference standard (#1235503; Sigma-Aldrich, St. Louis, MO). The endotoxin was shipped to the testing facility on dry ice and was maintained below −60°C for shipping and

Table 1. Treatment Assignment

Group	No. of Animals	Treatment (OU)	Dose (EU/eye)
1	3	Vehicle control (PBS)	0
2	2	Endotoxin	0.005
3	3	Endotoxin	0.02
4	4	Endotoxin	0.04
5	3	Endotoxin	0.08

below −70°C for freezer storage. Prior to reconstitution, the endotoxin was brought to ambient temperature by removal from the freezer 20 minutes prior to use. The 10,000 EU was reconstituted with 5 mL sterile phosphate-buffered saline (PBS) to a stock solution of 2000 EU/mL (Gibco #10010-023; Thermo Fisher Scientific, Waltham, MA). Certificate of analysis for the PBS confirmed endotoxin levels of <0.003 EU/100 µL. Following reconstitution, visual inspection was conducted to confirm that test formulations were clear solutions without any precipitates. Serial dilutions were subsequently performed using additional sterile PBS to achieve the desired dosing concentrations. All test article preparation prior to dosing was performed in a biosafety cabinet. Upon completion of dosing, the remaining endotoxin solutions were retained and stored in the freezer below −70°C.

Dosing

Monkeys received 100 µL intravitreal injections of endotoxin solution in both eyes (OU) on study day 0, in accordance with the treatment assignment (Table 1). For intravitreal dosing, 0.5% proparacaine was administered as a topical anesthetic and a Barraquer lid speculum was placed to facilitate access to the eye. Eyes were disinfected with 5% povidone–iodide (Betadine), then rinsed with 0.9% sodium chloride. Intravitreal injections were administered with a 0.3-mL insulin syringe with a 28-gauge 5/16-inch needle placed ∼2.5 mm posterior to the limbus at the level of the ora serrata in the inferior temporal quadrant, targeting the central vitreous. Topical neomycin–polymyxin B sulfates–bacitracin zinc ointment was applied after the injection. Monkeys in groups that received higher doses of endotoxin (groups 3 and 4) were administered 0.005 mg/kg buprenorphine IM twice a day for 48 hours following dosing to ameliorate potential pain associated with induced inflammation. No additional analgesics were required.

Paracentesis and Cytokine Analysis

Aqueous and vitreous humors were sampled at baseline and at day 7 by paracentesis. For the paracentesis procedures, eyes were prepared in the same method as intravitreal dosing, and a sterile 31-gauge needle with attached 0.5-mL syringe was placed 1 mm anterior to the limbus into the aqueous. The needle tip was advanced ∼6 mm into the aqueous chamber and 50 µL withdrawn into the syringe. Vitreous collection was performed immediately after aqueous taps; a sterile 30-gauge needle with attached 0.5-mL syringe was inserted into the vitreous chamber ∼2.5 mm posterior to the limbus. The needle tip was advanced 6 to 10 mm into the vitreous and 100 µL withdrawn into the syringe. Topical neomycin–polymyxin B sulfates–bacitracin zinc ointment was applied after the tap. Aqueous and vitreous samples were transferred to labeled cryotubes and stored below −70°C. These humor samples were evaluated at Trinity College Dublin, Ireland. A LEGENDPlex Non-Human Primate Inflammation panel (BioLegend, San Diego, CA) was used to assess levels of interleukin (IL)-6, IL-10, IL-1β, IL-12p40, IL-17A, interferon-β, IL-23, tumor necrosis factor α, interferon-γ, granulocyte macrophage colony-stimulating factor, IL-8, and chemokine ligand 2 (CCL2; also known as monocyte chemoattractant protein-1 [MCP-1]) using 50 µL of vitreous and 40 µL of aqueous per well. Negative control samples of aqueous and vitreous humor were collected from five untreated monkeys OU. Supernatant from monocytes treated with 10 ng/mL lipopolysaccharide for 24 hours was used for the positive control. The experiment was performed following the manufacturer's instructions, and samples were read using a BD LSR II Flow Cytometer (BD Biosciences, San Jose, CA). Data were analyzed using LEGENDPlex Data Analysis Software V8.0 (BioLegend).

Slit-Lamp Biomicroscopy

Slit-lamp biomicroscopy was performed OU for evidence of intraocular inflammation on study days 0, 1, 2, 4, 6, and 7. Evaluation of the posterior wall and vitreous was performed by posterior segment slit-lamp examination with a 90-diopter lens. All slit-lamp examinations were performed using a Zeiss 30 SL-M

slit-lamp biomicroscope (Carl Zeiss Microscopy, White Plains, NY). Scoring was applied to clinical ophthalmic findings using a nonhuman primate ophthalmic examination scoring system (see Supplementary Document S1) developed and adapted by Virscio from the Hackett–McDonald scoring scale, with summary clinical scores derived from the sum of individual components of the score. All slit-lamp examinations were performed by ophthalmology-trained MD or DVM investigators who had multiple years of training in slit-lamp examinations, including an MD ophthalmologist. Examiners were blinded to treatment groups while generating the slit-lamp biomicroscopic data. On study days 1, 2, 4, and 7, slit-lamp examinations were performed independently by two examiners. For all examinations with duplicate scores, the mean value of the scores was employed for clinical finding analysis. The duplicate scores were also evaluated to determine the inter-rater reliability of the applied ophthalmic examination scoring system.

Intraocular Pressure

Intraocular pressure (IOP) measurements were collected at each slit-lamp time point using a TONOVET tonometer (iCare Finland, Vantaa, Finland) set to the dog (d) calibration setting. When full sedation was achieved, animals were placed in a supine position for IOP measures with neck extended, head inverted, and the eye axis in the horizontal plane. Three measures were taken from each eye at each time point, and the mean values were employed for IOP analysis.

Ophthalmic Imaging

Ophthalmic imaging was performed at baseline and on study days 2 and 6 or 7. Prior to pupil dilation, measures of anterior chamber inflammation were performed using a Kowa FM-500 flare photometer (Kowa Company, Tokyo Japan) to measure Tyndall effect scattering of incident laser light by a photomultiplier tube and quantify anterior chamber flare as photon counts per millisecond. At each observation point, measurements were collected until seven acceptable readings (difference between two background measurements <15%) were obtained, the lowest and highest readings were deleted, and the mean value ± the standard deviation (SD) was calculated, as specified by the manufacturer.

Topical mydriatics, including 10% phenylephrine, 1% tropicamide, and 1% cyclopentolate, were applied prior to the fundus imaging. Bilateral color fundus images of the retina were captured with 50 degrees of view centered on the fovea using a TOPCON TRC-50EX retinal camera (TOPCON Corporation, Tokyo, Japan) with Canon EOS 6D digital imaging hardware (Canon, Inc., Tokyo, Japan) and NewVision Fundus image analysis system software. Color images of the anterior segment of the eye were also obtained at the time of fundus photography. OCT and confocal scanning laser ophthalmoscopy (cSLO) were performed using SPECTRALIS HRA-OCT with eye tracking (Heidelberg Engineering, Heidelberg, Germany) and Heidelberg HEYEX image capture and analysis software. The cSLO infrared and autofluorescence retinal images were obtained using the 30° lens followed by an overall volume scan of the entire macula, which was performed at a dense scan interval. Retinal cross-sectional display images were qualitatively assessed. Additionally, prior to pupil dilation, anterior segment SPECTRALIS imaging was performed at the iridocorneal angle with infrared cSLO and OCT images of the anterior segment.

Histopathology

One animal with representative inflammation from the 0.04-EU/eye dosing group was selected for histopathology on day 2 (the remaining monkeys were returned to the colony following confirmation of good ocular and overall health). The monkey was euthanized with ketamine (8–10 mg/kg IM) followed by sodium pentobarbital (25–30 mg/kg intravenously). Prior to euthanasia, aqueous and vitreous paracentesis was performed as previously described. Each globe was enucleated, excess orbital tissue was trimmed, and the eyes were placed in Davidson's solution for 24 hours and stored at 2° to 8°C. At 24 hours, eyes were transferred to PBS with 0.05% azide and stored and shipped at 2° to 8°C. Histopathology was performed at StageBio (Mount Jackson, VA). The globes were processed, embedded in paraffin, sectioned, and stained with hematoxylin and eosin (H&E). Three transverse step sections (4–6 µm thick and approximately 100 µm apart) were generated from each globe and included the optic nerve and macula.

Statistical Analysis

Statistical analysis was performed on the slit-lamp examination data to compare between-group cumulative scores, as well as select individual inflammatory parameters. Friedman's test for nonparametric, nonlinear ordinal data was applied with Dunn's multiple-comparison post hoc test to compare between treatment groups. To determine if changes in aqueous flare measurement were significant, the baseline

measurements were compared to day 2 and day 7 for each group using a paired, two-tailed *t*-test. Statistical level of significance was set at $\alpha = 0.05$ (Prism 7; GraphPad, San Diego, CA). The change in cytokine levels between time points was assessed using the paired Wilcoxon signed-rank test, and two-way analysis of variance (ANOVA) was used to assess differences between treatment groups. To assess the inter-rater reliability of the applied ophthalmic examination scoring system, 94 examinations were performed in duplicate, each performed by two of three different examiners. For each examination, 21 parameters were scored, and the scores were compared between examiners. Both individual parameter score comparisons and cumulative examination score comparisons were performed to establish inter-rater reliability, reported as percentages.

Results

Intravitreal dosing was successfully performed in accordance with Table 1. There was no sign of persistent vitreous leakage following dosing on day 0. No signs of injection-associated ocular injury or endophthalmitis were observed following intravitreal injection. Twice daily cage-side observations revealed no clinical signs indicative of systemic test article–related adverse effects or inadequately managed ocular discomfort. IOP measurements in all groups remained within normal range throughout the study (10–22 mmHg).

Slit-Lamp Biomicroscopy Findings

On day 1 following dosing, a dose-related inflammatory response was observed in all groups. The vehicle group showed a mild inflammatory response that largely resolved by day 7. The inflammatory response induced by 0.005 EU/eye did not exceed that of the vehicle. Inflammation peaked on day 2, with the highest inflammatory response observed in the 0.04-EU/eye group, followed closely by the 0.08-EU/eye group; however, the 0.08-EU/eye group demonstrated the highest sustained inflammatory response throughout in-life observation. By day 18, minimal inflammation was observed (Fig. 1), and all active inflammation had resolved by day 25.

Aqueous cell infiltration was observed in all groups as early as day 1 to a dose-dependent extent. Aqueous cell presence peaked for the highest dose group on day 1 and for all other groups on day 2 and had cleared in all but one monkey by day 18. The transient infiltration of few aqueous cells observed in the vehicle group was likely in response to the intravitreal dosing procedure, and no additional cellular response was observed in the 0.005-EU/eye dosing group (Fig. 2).

The vitreous cell response was similar, although delayed in comparison to the aqueous cell response.

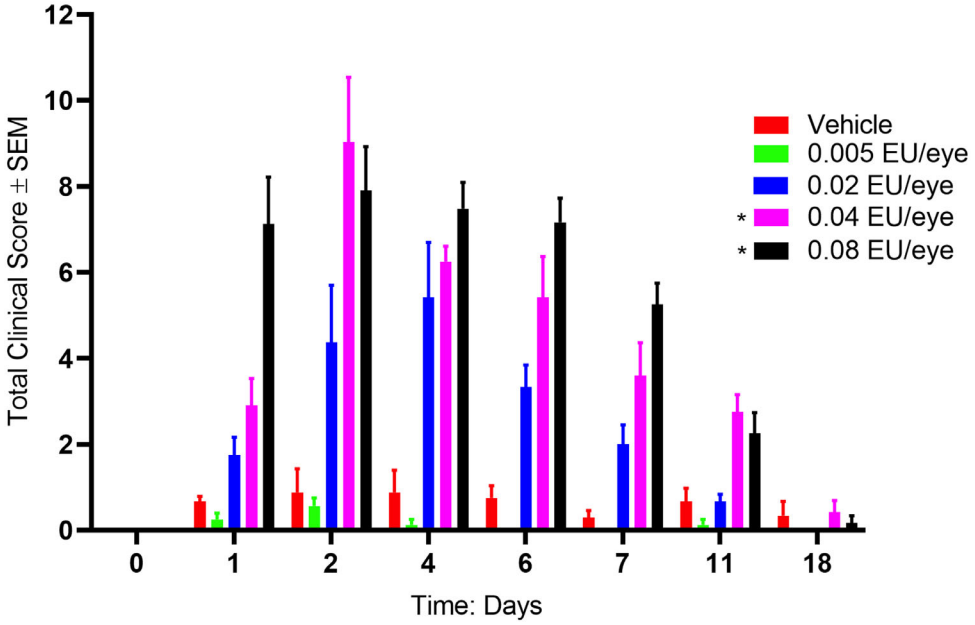

Figure 1. Dose-related inflammatory response of mean cumulative ophthalmic clinical scores, with *error bars* indicating standard error of the mean (SEM). Analysis of non-parametric data demonstrated that doses exceeding 0.02 EU/eye induced pathologic clinical scores significantly greater (*) than the vehicle over time (0.04 EU/eye, $P = 0.0423$; 0.08 EU/eye, $P = 0.0139$).

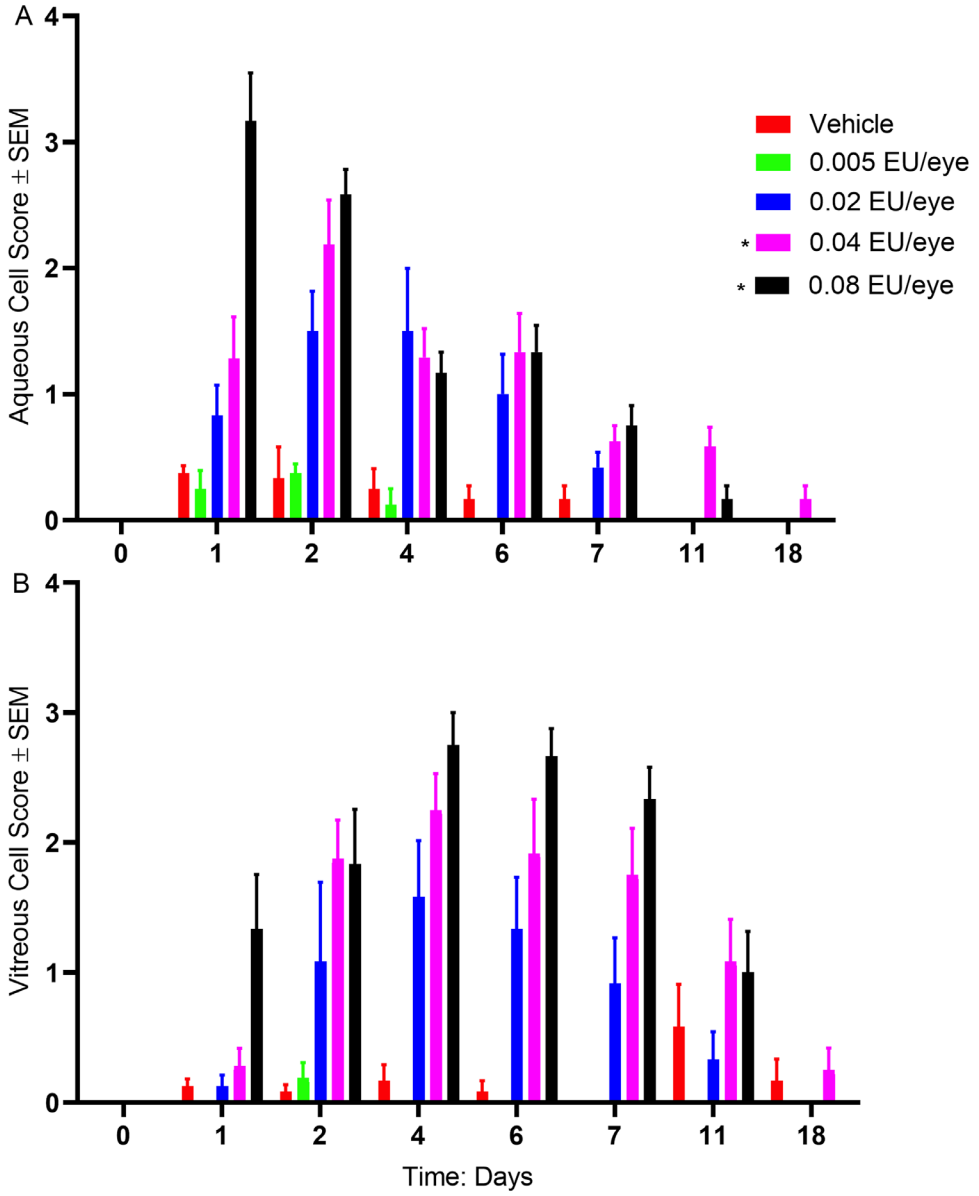

Figure 2. (A) Dose-related mean aqueous cell response beginning on day 1 and resolving by day 18. *Error bars* indicate SEM. Analysis of non-parametric data demonstrated that doses above 0.02 EU/eye induced an aqueous cell score significantly greater (*) than the vehicle over time (0.04 EU/eye, $P = 0.0325$; 0.08 EU/eye, $P = 0.0186$). (B) Dose-related mean vitreous cell response beginning on day 1 and resolving by day 18. Analysis of non-parametric data demonstrated that doses above 0.02 EU/eye induced a vitreous cell score significantly greater (*) than the vehicle over time (0.04 EU/eye, $P = 0.0247$; 0.08 EU/eye, $P = 0.0076$).

Cell infiltration into the vitreous was initially observed at day 1 but peaked at day 4. Vitreous cells, scored as "few," were observed in the vehicle group, again likely in response to the intravitreal dosing procedure; no additional vitreous cell infiltration was induced by the 0.005-EU/eye dose. After the vitreocentesis procedures performed following day 7 examinations, many erythrocytes were observed in the vitreous of one vehicle monkey (B289). As this monkey demonstrated minimal inflammation at all time points post-dosing with no inflammation observed on day 7 (score of 0 OU), this cellular response was attributed to a complication of the vitreocentesis procedure (Fig. 2).

Iris hyperemia was observed in doses exceeding 0.02 EU/eye, beginning on day 1 and remaining stable through day 11. All iris hyperemia resolved by day 18, and none was observed in the vehicle, 0.005-EU/eye, or 0.02-EU/eye dose groups. Iris hyperemia scores at 0.08 EU/eye were significantly greater than for the vehicle ($P = 0.0104$).

Keratic precipitates on the corneal endothelium were observed in all groups, with the highest numbers

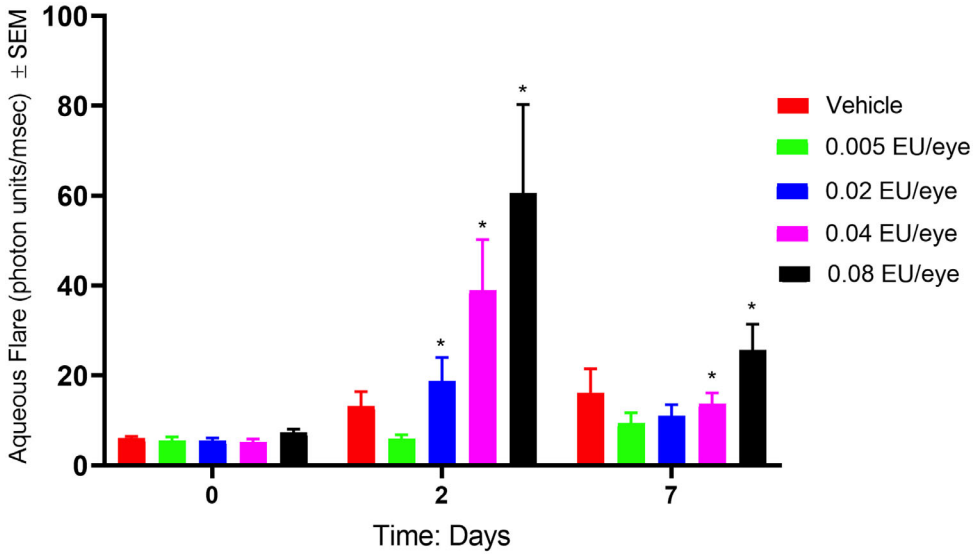

Figure 3. Mean laser flare photometry measures. *Error bars* indicate SEM. Statistical analysis was performed by comparison of baseline measurements on day 2 and day 7 for each group using paired, two-tailed *t*-tests. *Significant results.

observed in doses exceeding 0.02 EU/eye, beginning on day 1 and mostly resolving by day 18. Differences in keratic precipitate scores among treatment groups were not statistically significant, although 0.02 EU/eye and 0.08 EU/eye trended toward significance (0.02 EU/eye, $P = 0.0548$; 0.08 EU/eye, $P = 0.0705$). Anterior chamber fibrin strands and small consolidated fibrin masses were observed in doses exceeding 0.005 EU/eye, beginning on day 1 and resolving after day 7. No fibrin was observed in the vehicle group or the 0.005-EU/eye dose group. Anterior and posterior lens capsule deposits were observed, correlating with aqueous and vitreous cell infiltration. These deposits were mild and did not obscure the view of the fundus. Transient aqueous flare was detectable by slit-lamp examination in some animals in the higher

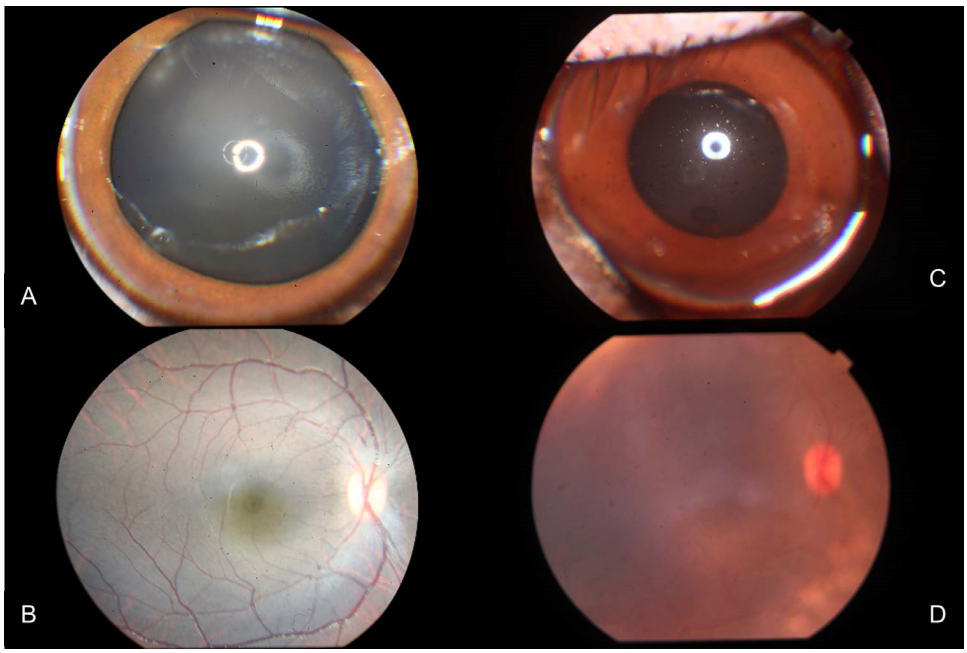

Figure 4. Representative anterior segment (A) and color fundus (B) images obtained from monkey B205 OD (high dose group, 0.08 EU/eye) at baseline with a pupil diameter of 8 mm and a slit-lamp cumulative clinical score of 0. Representative anterior segment (C) and color fundus images (D) obtained from the same eye on day 2 with a pupil diameter of 5 mm and a slit-lamp cumulative clinical score of 8.75.

Table 2. Retinal Thickness Measurements at Baseline and Post-Dosing

Time Point	Minimum (µm)	Maximum (µm)	Average (µm)	SD	95% CI
Baseline	294.4	374.4	337.9	17.4	331.7–344.1
Day 2	299.8	376.6	343.3	18.3	336.8–349.9
Day 7	302.1	396.2	345.3	24.5	336.3–354.4

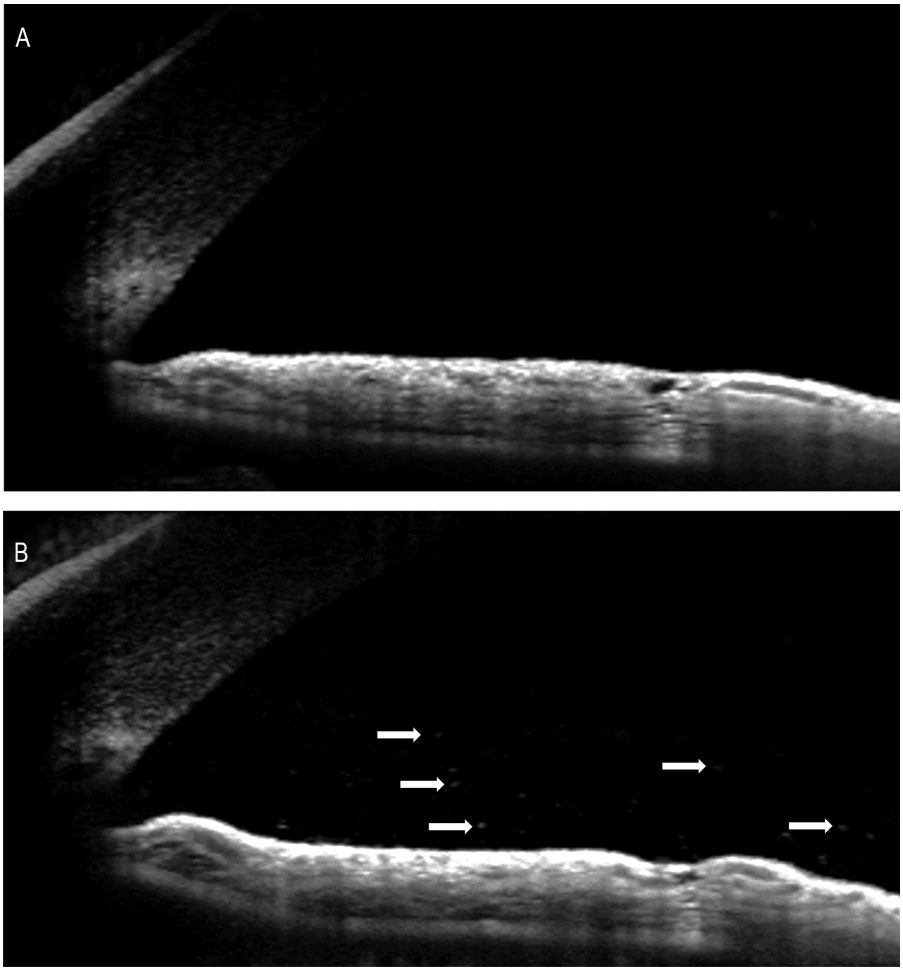

Figure 5. Representative anterior segment OCT images of iridocorneal angle from group 5 monkey (0.08 EU/eye). (A) Baseline OCT image. (B) Day 2 image with visible cells in the anterior chamber (*arrows*).

dosing groups (0.04 and 0.08 EU/eye) on days 1 and 2. Other findings included corneal epithelial defects, surface dryness, and mild corneal edema.

Flare Photometry

Laser flare measures were obtained from all eyes, although corneal surface irregularities and corneal edema contributed to technical variability. Peak laser flare measures were observed at day 2 in all endotoxin-treated eyes, with the highest readings observed in the 0.04-EU/eye and 0.08-EU/eye dose groups (Fig. 3). A significant increase in aqueous flare measurements was observed in the 0.02-, 0.04-, and 0.08-EU/eye groups on day 2 (0.02 EU/eye, $P = 0.0485$; 0.04 EU/eye, $P = 0.0188$; 0.08 EU/eye, $P = 0.0446$), and they were still significantly increased in the two highest dose groups on day 7 (0.04 EU/eye, $P = 0.0258$; 0.08 EU/eye, $P = 0.034$).

Color Fundus Photography

CFP conducted for all groups revealed no changes in retinal morphology or vasculature over the 25 days of in-life examinations. Decreased fundus image quality,

however, was observed in all dose groups at day 2 and day 7 secondary to anterior segment changes and reduced mydriasis (Fig. 4). Day 2 images in the higher dose groups (0.04 and 0.08 EU/eye) revealed greater fundus image blurring and obscuration on day 2 than in the lower dose groups.

Optical Coherence Tomography

SPECTRALIS OCT and cSLO images revealed no obvious changes in retinal morphology over the course of the study. Retinal volume and thickness measures derived from OCT images increased marginally from baseline to post-dosing measurements; however, no dose-related trend was observed (Table 2). Mild retinal pathology was observed on day 2, including slight wrinkling in the parafoveal inner limiting membrane (ILM) in select animals in groups 4 and 5 (0.04 EU/eye and 0.08 EU/eye, respectively). As with the color fundus imaging, the quality of the posterior OCT images obtained decreased for all groups on day 2 and day 7. In anterior segment OCT images, aqueous cells were visible in eyes for which the aqueous cell score was 2 and higher, equating to at least 11 to 20 cells per slit beam of 3 × 1 mm (Fig. 5). Vitreous cells were similarly visible in posterior segment OCT images for most eyes in which the vitreous cell score was 2 or higher, equating to at least 11 to 20 cells per slit beam of 3 × 1 mm (Fig. 6). Media clarity and achievable image quality, however, greatly impacted the visibility of vitreous cell; in eyes with poor dilation, corneal surface dryness, or abundant anterior chamber pathology, the posterior segment OCT image quality was greatly reduced, and vitreous cells were no longer discernable. Additionally, retinal images were blurred with decreased resolution and achievable retinal layer segmentation.

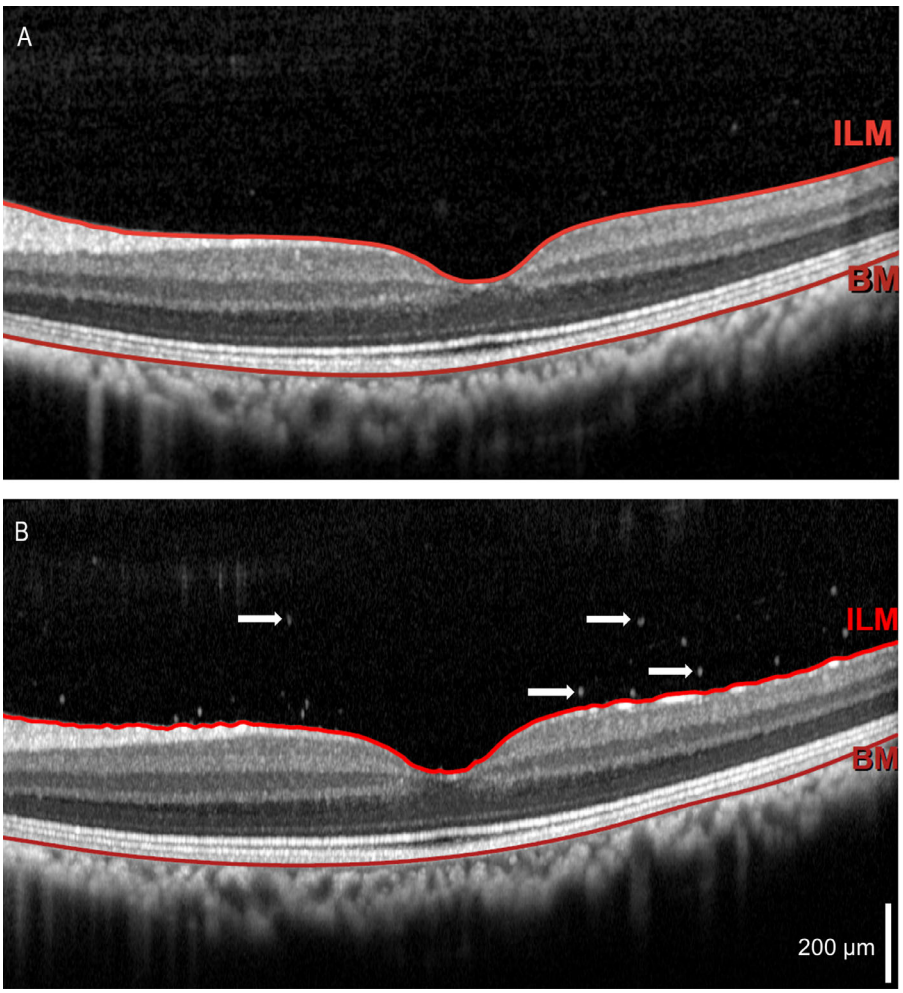

Figure 6. Representative posterior segment images from group 5 (0.08 EU/eye). (A) Baseline OCT posterior segment image. (B) Day 2 image, with visible cell in vitreous humor (*arrows*). Mild retinal pathology was observed on day 2, including slight wrinkling in the parafoveal ILM in some animals in groups 4 and 5 (0.04 EU/eye and 0.08 EU/eye, respectively). BM, basement membrane.

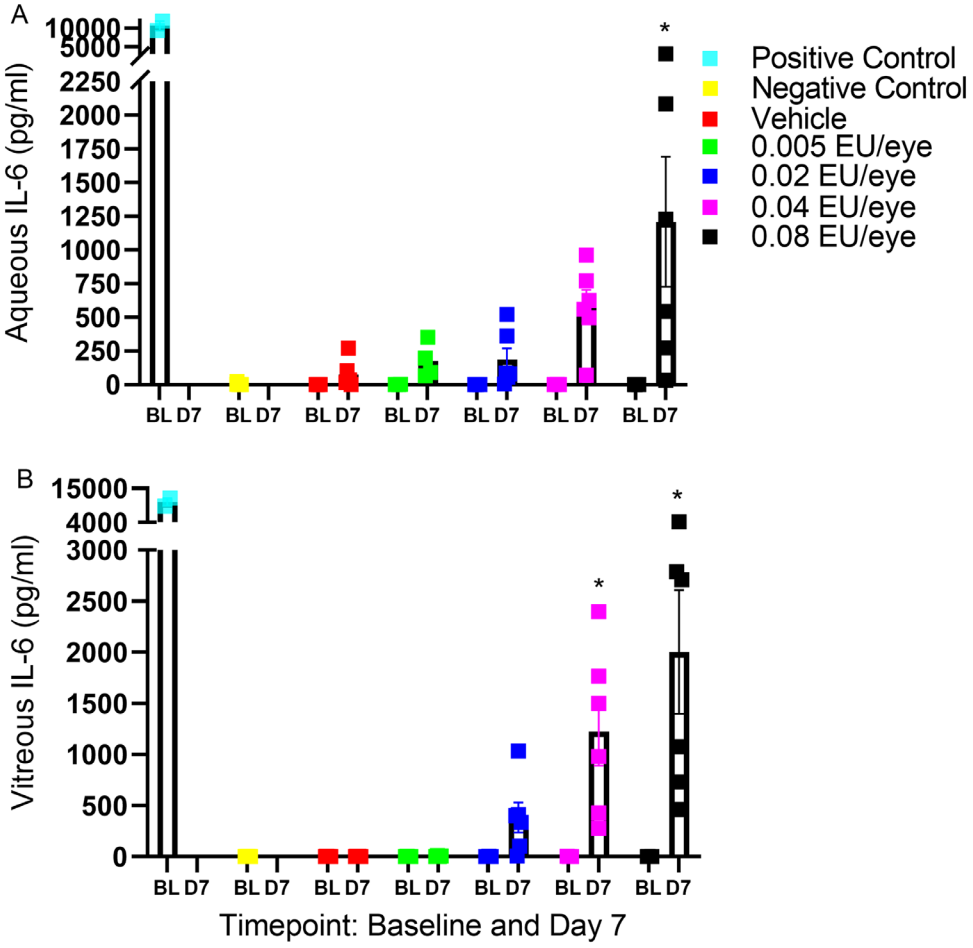

Figure 7. IL-6 cytokine levels in aqueous humor (A) and vitreous humor (B) collected at baseline and on day 7. *Error bars* represent the SEM. Two-way ANOVA was used to assess differences between the vehicle and treatment groups. *Significant results.

Aqueous Humor and Vitreous Cytokine Analyses

On day 7, there was a significantly elevated IL-6 level in the aqueous humor for the 0.08-EU/eye group when compared to the vehicle ($P = 0.0002$) and a significant increase in IL-6 levels in the vitreous of the 0.04-EU/eye and 0.08-EU/eye groups when compared to the vehicle ($P = 0.0048$ and $P < 0.0001$, respectively) (Fig. 7). Similarly, there was a significantly elevated MCP-1 level in the aqueous humor for the 0.04-EU/eye group when compared to the vehicle ($P = 0.0412$) and a significant increase in MCP-1 levels in the vitreous for the 0.02-EU/eye, 0.04-EU/eye, and 0.08-EU/eye groups when compared to the vehicle ($P < 0.0001$, $P < 0.0001$, and $P = 0.0412$, respectively) (Fig. 8). A trend toward significance was seen for MCP-1 increases in the aqueous humor for the highest dosing group when compared to the vehicle (0.08 EU/eye, $P = 0.0531$). Cytokine levels in the one animal in group 4 (0.04 EU/eye) sampled on day 2 (at euthanasia) were markedly higher than for the rest of the group sampled on day 7, particularly for cytokines IL-6, IP-10, IL-8, and MCP-1 (Fig. 9).

Histopathology

Histopathology for the pair of 0.04-EU dosed eyes revealed microscopic findings in both eyes (OU) and included minimal mononuclear cell infiltration within the aqueous humor (OU), minimal (left eye, OS) to mild (right eye, OD) mononuclear cell infiltration within the vitreous humor, mild fibrin within the aqueous and vitreous humors (OU), and minimal corneal pigmentation (OD only) (Fig. 10). Nominal mononuclear cell infiltration in the aqueous humor was characterized by low numbers of macrophages and lymphocytes free within the anterior chamber, immediately subjacent to the corneal endothelium. Cellular infiltrates were admixed with minimal eosinophilic beaded fibrillar strands (fibrin). Mild mononuclear cell infiltration within the vitreous resembled the

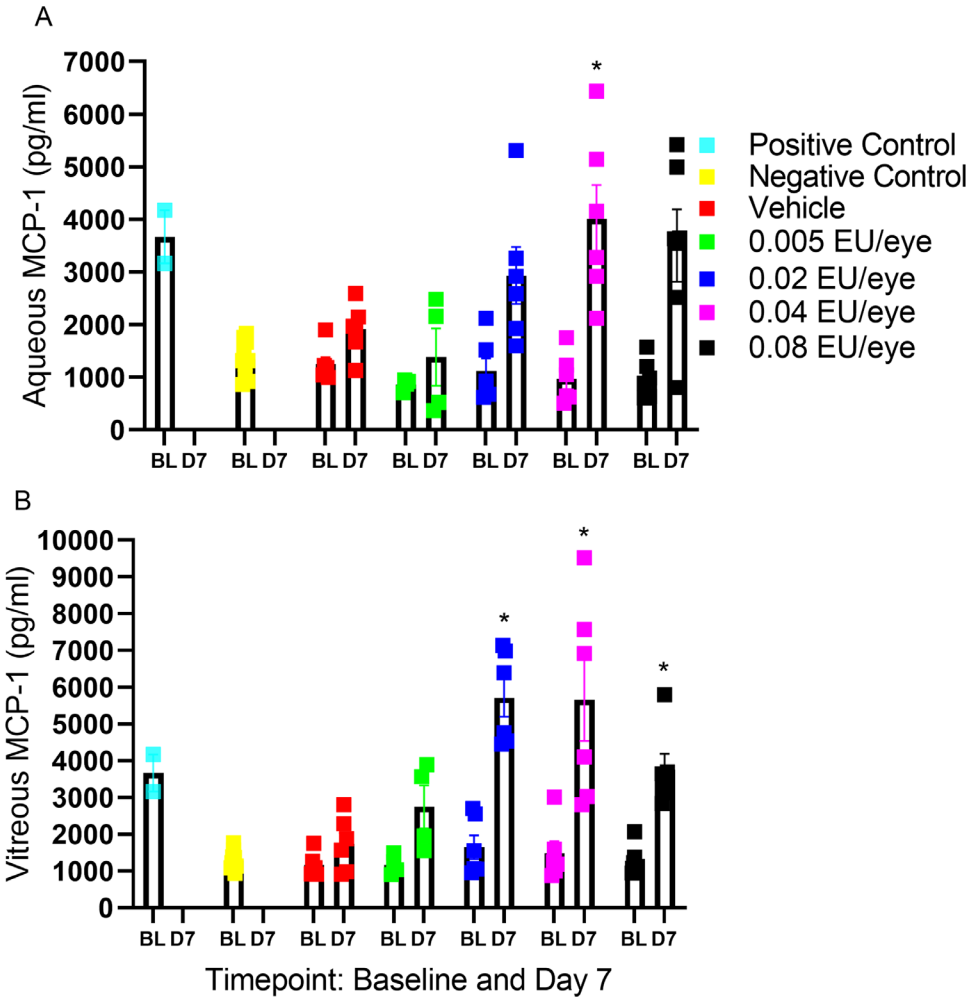

Figure 8. MCP-1 cytokine levels in aqueous humor (A) and vitreous humor (B) collected at baseline and on day 7. *Error bars* represent the SEM. Two-way ANOVA was used to assess differences between the vehicle and treatment groups. *Significant results.

infiltrates described in the aqueous humor. Cellular infiltrates were most frequently observed within the anterior vitreous and were admixed with minimal fibrin. Corneal pigmentation (OD only) was characterized by a locally extensive area of perilimbal corneal epithelial cells (extending <1 mm from the limbus) containing intracellular brown (melanin) granules. In the affected area, melanin granules were observed in all corneal epithelial layers and were associated with vacuolation of the intermediate and superficial epithelial cells.

Inter-Rater Reliability of Virscio Nonhuman Primate Ophthalmic Examination Scoring System

For the inter-rater reliability of the applied green monkey slit-lamp examination scoring system, the minimum possible cumulative summary score for an ophthalmic examination was 0, and the maximum possible cumulative summary score was 73. The minimum reported cumulative summary score was 0, and the maximum reported cumulative summary score was 16.5. Both individual parameter score comparisons and cumulative examination score comparisons were performed to establish inter-rater reliability, reported as percentages (Table 3).

Discussion

The current study was conducted to investigate the dose-dependent inflammatory response and NOAEL following a single intravitreal dose of endotoxin in the African green monkey. Overall, the inflammatory response observed was self-limiting within the

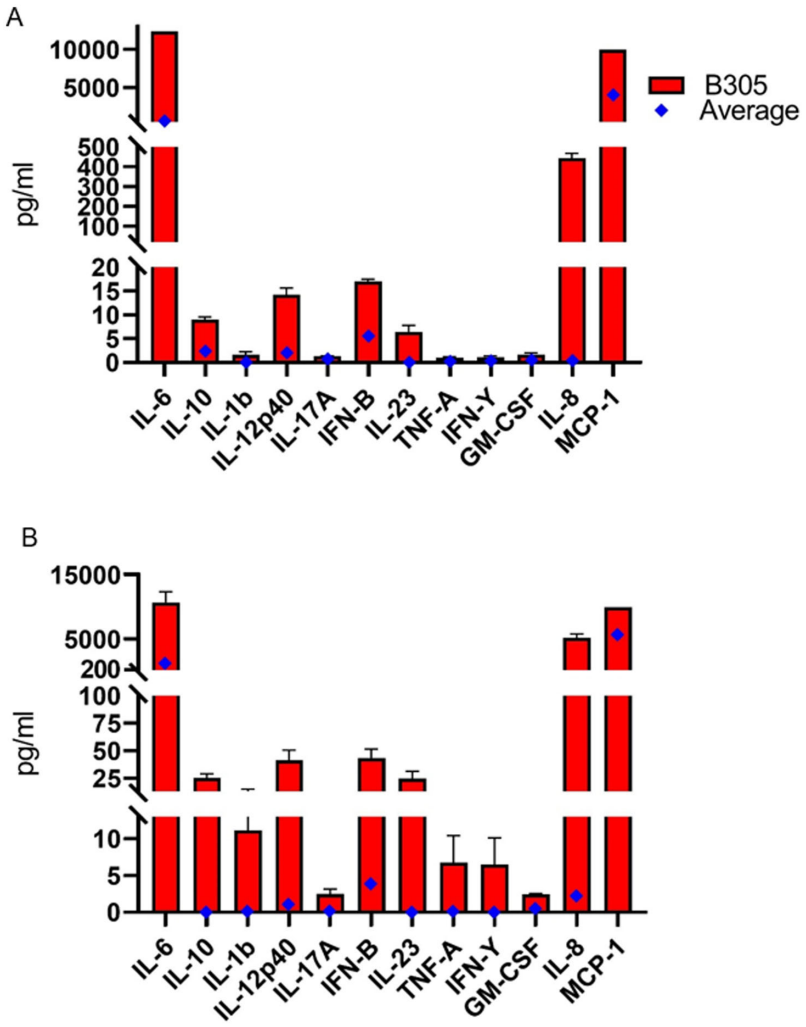

Figure 9. Aqueous (A) and vitreous (B) cytokine levels for monkey B305 (*red*) sacrificed at day 2 with average cytokine levels in eyes treated with 0.04 EU/eye at day 7 (*blue*), demonstrating comparatively elevated levels in the samples collected on day 2 for most evaluated cytokines. *Error bars* represent the SEM.

Table 3. Inter-Rater Reliability of Virscio Nonhuman Primate Ophthalmic Examination Scoring System

	Individual Parameter Scores ($N = 1939$)		Cumulative Examination Scores ($N = 94$)	
Score Difference	%	*n*	%	*n*
None	91.0	1764	25.5	24
≤0.5	95.6	18549	50.0	47
≤1	99.2	1923	71.3	67
≤2	99.9	1938	87.2	82
≤3	100	1939	94.7	89

low endotoxin doses explored. Although the results demonstrated that the average total inflammation score was slightly higher in the 0.04-EU/eye group than in the 0.08-EU/eye group on day 2 (average score of 8 vs. score of 9) (Fig. 1), the 0.08-EU/eye dose had the most sustained total inflammation over the successive observation periods. In our experience evaluating ocular inflammation in the green monkey, these results are consistent with the degree of data scatter observed in response to a given test article, reflecting individual animal and eye biological variability. All inflammation resolved without antiinflammatory

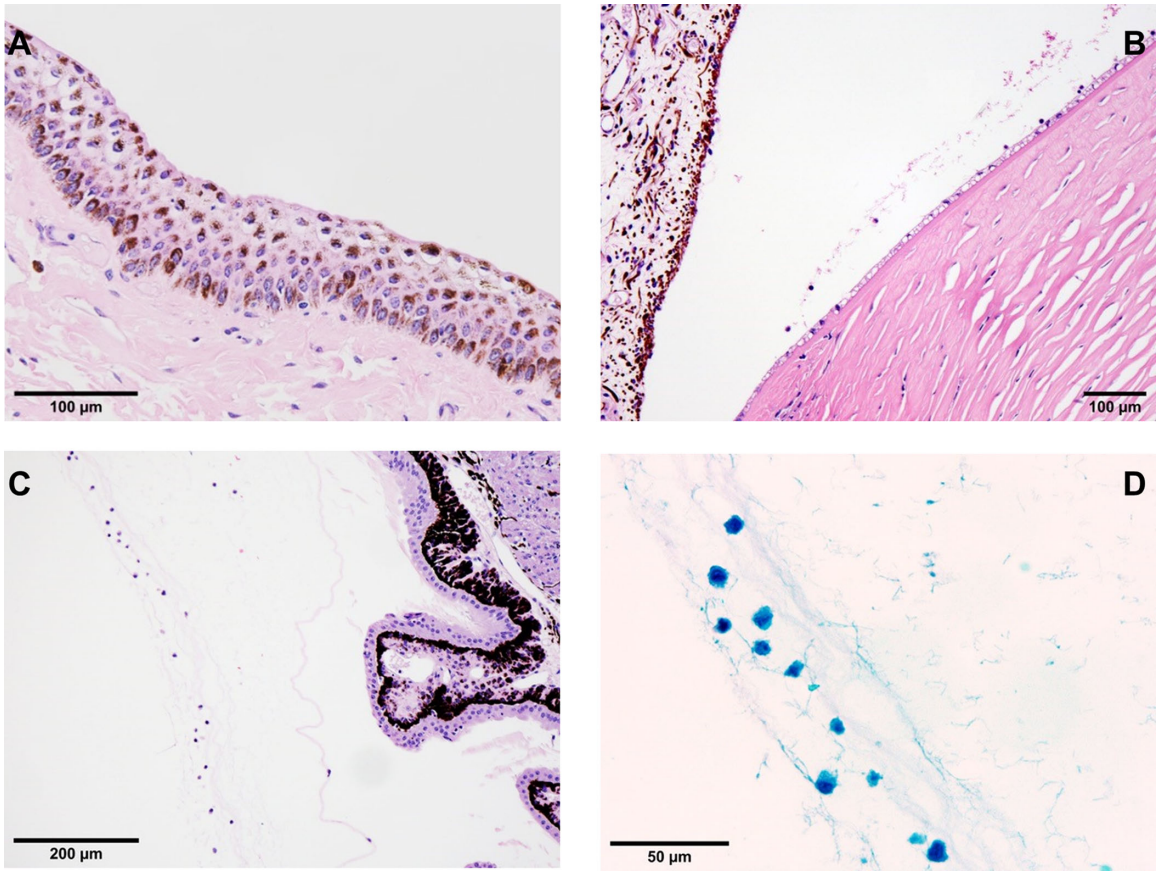

Figure 10. Photomicrographs of H&E-stained sections of the globes from monkey B305. Microscopic findings included a locally extensive area of perilimbal corneal epithelial pigmentation OD (A) and minimal to mild mononuclear cell infiltrates admixed with fibrin in both eyes (OD depicted) in the anterior chamber (B) and vitreous (C). (D) Higher magnification image of the mononuclear cell infiltrates showing that the majority of cells were macrophages.

intervention, and most active inflammation, including the more transient aqueous cell, flare, and fibrin, resolved within the first 10 days. Vitreous cell and keratic precipitates, which can take longer to clear from the eye, were present for approximately 3 weeks. These results support the value of minimizing endotoxin contamination in test or tool compounds administered intraocularly to avoid confounding the interpretation of ophthalmic examination results and determination of safety. They further suggest that, if a significant inflammatory response persists beyond 2 weeks or continues to worsen beyond the first week, then the etiology is unlikely endotoxin contamination within the dose range we have evaluated and more likely an adverse effect of the test article itself. Similarly, a delayed inflammatory response that does not begin within 24 to 48 hours after dosing suggests an alternative etiology. For example, in our experience, a mild and transient inflammatory response can be observed in the first week following administration of adeno-associated virus (AAV) gene-therapy candidates. The timing for transduction and gene expression can vary with different AAV vector constructs, and inflammation that emerges 2 weeks after dose administration is likely attributable to gene expression and an inflammatory response to the gene product.

Only mild retinal pathology was observed with mild wrinkling of the ILM in some animals from the higher dose groups (0.04 and 0.08 EU/eye), and retinal volume and thickness measures increased only marginally from baseline to post-dosing evaluations with no dose-related trend observed; however, serial sedation and ophthalmic imaging procedures, in addition to endotoxin dose administration, resulted in decreased pupil diameter, corneal dryness, and intraocular pathology that reduced the quality of CFP and OCT images. The average pupil size reduced equally across all groups throughout the study; the smallest pupil diameters were observed on day 6 (average 5 mm compared to 7.75 mm at baseline)

and had not fully recovered by day 18 (average 6.43 mm). As an equal reduction in pupil diameter was observed in all groups, this change was likely secondary to corneal dryness and associated mild irritation in the setting of sedation for examination and resulting decreased response to mydriatics rather than a response to endotoxin. Reduced pupil size contributed to decreased image quality during posterior chamber visualization and imaging. An additional contributor to decreased media clarity was the corneal pigmentation triggered by povidone–iodide exposure and subsequent sedation cycles. Decreased image clarity can impact quantitative evaluation of ophthalmic studies, such as in fluorescein angiographic evaluation of leakage modulation in models of wet macular degeneration. Certain strategies can be employed to minimize the impact of corneal surface dryness and irritation on image quality, including minimizing the duration of sedation for ophthalmic examinations, the application of lubricating eye drops and saline throughout imaging procedures, and the application of lubricating eye ointment for sedation recovery after examinations. Additionally, minimizing 5% povidone–iodine contact time to as low as 30 seconds for dosing and paracentesis procedures can still achieve significant reduction of bacterial presence while decreasing the level of induced corneal surface and conjunctival irritation.[21] In this study, despite the implementation of these practices, the frequent sedations and ophthalmic examinations necessary to evaluate inflammatory endpoints contributed to corneal surface dryness and subsequent reduction of image quality reduction. Additionally, miosis associated with iris irritation can also reduce the quality of posterior segment images. Antiinflammatory therapy can facilitate pupil response to mydriatics; however, some pupils remain refractory to dilation regardless of antiinflammatory therapy, contributing to poor posterior segment images and impacting study interpretation.

The histopathology analysis of the 0.04-EU dosed eyes closely correlated with slit-lamp examination findings, which included minimal to mild monocytic keratic precipitates on the corneal endothelium, moderate to marked aqueous cells, mild aqueous flare, mild fibrin strands (OS), and mild (OS) to moderate (OD) vitreous cells, in addition to mild corneal pigmentation. There were no microscopic correlates for the ophthalmic clinical examination results of iris hyperemia or anterior lens capsule deposits. All microscopic observations were considered non-adverse due to limited severity and a lack of clinical evidence suggestive of functional impairment or irreversible change. Therefore, the inflammation induced by 0.04 EU/eye in this monkey, although detectable at slit-lamp examination, did not have a durable deleterious effect on eye health, suggesting that the long-term impact of endotoxin contamination at this level is minimal. This level of endotoxin contamination, however, would still confound results in the safety evaluation of candidate therapeutics or devices and prevent differentiation between the endotoxin contaminant or the test article or device as a possible etiology to detected inflammatory response.

Results reported in the cynomolgus macaque included mild microscopic findings that were detected in eyes dosed with ≥0.21 EU and collected on day 15, a time point after resolution of most clinical examination findings.[5] We detected similar microscopic changes at the lower level of 0.04 EU in eyes collected on day 2 at the peak of inflammation following endotoxin administration. It may have been the case that, had eyes been collected at peak inflammation in the cynomolgus macaque study, microscopic changes would have been detected at a lower dose, similar to our findings in the green monkey. We performed this study to evaluate the interspecies differences between cynomolgus and green monkeys in response to a known canonical inflammatory agent. This question is of recurring relevance to the interpretation of ophthalmic therapeutic and device candidate safety data generated in respective test systems. Referencing the work in cynomolgus monkeys, we elected to evaluate the lower end of the dosing range, for which antiinflammatory intervention was not necessary to maintain animal welfare. Overall, our dose-dependent response was similar to that seen in the cynomolgus macaques, with similar trends for most inflammatory pathologies evaluated. Although acknowledging technical and methodological differences among the study designs, these findings confirm our hypothesis that green monkeys are as sensitive to intravitreal endotoxin as cynomolgus macaques and rabbits.[4,5]

Although we did not observe a statistically significant inflammatory response in the 0.02-EU/eye treated group versus vehicle control, mild to moderate inflammation was observed. Only the 0.005-EU/eye group exhibited no inflammation greater than vehicle, defining the NOAEL. Mild, transient cellular inflammation following dose administration was observed in all groups, including the vehicle group. These findings differ from the cynomolgus study, in which zero inflammation was reported for the vehicle group and the 0.01-EU/eye group. No statistics were reported in the cynomolgus study for comparison. A reason for this difference in sensitivity between the green monkey and the cynomolgus monkey may be a true interspecies difference; however, it is also possible that our slit-lamp biomicroscope equipment had greater sensitivity,

as well as potentially greater clarity and illumination, leading to increased sensitivity to mild inflammation. The equipment utilized in the cynomolgus study was not specified.[5]

An additional contributor to the greater sensitivity of the green monkey test system in this study may be the applied nonhuman primate ophthalmic examination scoring system (see Supplementary Document S1). Adapted from the Hackett–McDonald scoring scale and Nussenblatt Scale for vitreous haze, this scoring scale has been tailored to the inflammatory response observed in the African green monkey eye.[15–20] Significant enhancements include increased stratification (and resulting sensitivity) for the quantification of aqueous and vitreous cells, addition of scores for keratic precipitates and anterior and posterior lens capsule deposits, and differentiating scores for anterior chamber fibrin from aqueous flare. This scale has allowed finely graded evaluation of discrete inflammation signs in the green monkey eye, with added ability to distinguish degrees of inflammation. We also included half scores in many categories, thus allowing for the documentation and quantification of very mild inflammatory changes. The added granularity of our scoring system may account for the detection of mild inflammation after intravitreal vehicle administration in the green monkey that was not reported in the cynomolgus macaque.[2] Our nonhuman primate scoring system additionally has high inter-rater reliability, with 99.2% likelihood of individual parameter scores differing by 1 or less and 87.2% likelihood of cumulative scores differing by 2 or less, when used by appropriately trained practitioners. These results indicate a high level of reproducibility in collected data when trained staff, high-quality ophthalmic equipment, and a detailed validated ophthalmic examination scoring system are utilized.

Cytokine evaluation of endotoxin-induced inflammation 1 week after dose administration revealed significant dose-related elevations in IL-6 and MCP-1 cytokines. IL-6 is a proinflammatory cytokine secreted by a variety of cells, including macrophages, that has been defined as a key factor in uveitis in humans.[22] IL-6 has additionally been demonstrated to act as the primary cytokine involved in endotoxin-induced uveitis in mice and rats.[23–25] MCP-1 (also known as CCL-2) is key for recruitment of leukocytes to sites of inflammation[26] and has similarly been shown to play an important role in uveitis in humans,[22] as well as in the endotoxin-induced uveitis rat model.[23] The levels of IL-6, IP-10, IL-8, and MCP-1 cytokines in two eyes collected on day 2 were markedly higher than those on day 7 for other eyes in the same group. This finding, when considered in association with clinical examination scores, is suggestive of higher cytokine levels for other animals had they been sampled at day 2. Generating these data was not pursued in this study, as we did not want to introduce a confounding inflammatory effect by performing paracentesis procedures at the time of peak endotoxin inflammatory response on day 2. One important procedural consideration is that, due to volume limitations for non-terminal aqueous and vitreous sample collections in animal models, we elected not to run the cytokine analyses in technical duplicate. The LEGENDPlex nonhuman primate inflammatory panel requires a minimum sample volume of 12.5 µL per well, but we elected to use the full 50-µL samples available for both aqueous and vitreous analysis. This volume yielded a detectable, but low, level of response for most cytokines, and smaller sample volumes may have prohibited this detectable response. A limitation of this study is that endotoxin levels in test article dilutions were not tested for exact endotoxin content. Additionally, low concentrations of endotoxin in the vehicle PBS itself (specified to be <0.003 EU/100 µL) may have affected tested and reported endotoxin levels.

In conclusion, we report a dose-dependent inflammatory response to intravitreal endotoxin in the African green monkey with inflammation peaking on day 2 and substantially resolving by day 18. The NOAEL for intravitreal endotoxin in the green monkey was near 0.005 EU/eye; statistically significant inflammation was observed for doses higher than 0.02 EU/eye, and microscopic findings were detectable at 0.04 EU/eye. These data indicate that endotoxin levels as low as 0.02 EU/eye can cause moderate inflammation in the African green monkey eye and that candidate therapeutic compounds should be confirmed to have endotoxin levels below this threshold prior to safety testing to avoid confounds to the assessment of inflammation as a safety endpoint and minimize impact on animal welfare. We also report a nonhuman primate ophthalmic scoring system that achieves high sensitivity and inter-rater reliability for the quantification of mild to severe inflammation in the nonhuman primate eye.

Acknowledgments

The authors thank Aryamitra Banerjee for her helpful discussion of the study design. We also thank the technical research and veterinary teams at Virscio for their contributions to the study execution; Virscio employees provided commercial nonhuman primate translational research services.

Supported by Virscio, Inc.

Disclosure: **T.M. Corey**, Virscio (E); **V.V. Woodley**, Virscio (E); **M. O'Connor**, Virscio (E); **E. Connolly**, Trinity College Dublin (E); **S. Doyle**, Virscio (F), Trinity College Dublin (E); **S. Shrader**, Virscio (F), HSRL (E); **C. Phipps**, Virscio (E); **K. Isaac**, Virscio (E); **M. Lawrence**, Virscio (I, S, E)

References

1. Lerouge S. Introduction to sterilization: definitions and challenges. In: Simmons A, ed. *Sterilisation of Biomaterials and Medical Devices*. Cambridge, UK: Woodhead Publishing; 2012:1–19.
2. Dawson M. Endotoxin limits for parenteral drug products. *BET White Paper*. 2017;1(2):1–7.
3. Csukas S, Paterson CA, Brown K, Bhattacherjee P. Time course of rabbit ocular inflammatory response and mediator release after intravitreal endotoxin. *Invest Ophthalmol Vis Sci.* 1990;31(2):382–387.
4. Bantseev V, Miller PE, Bentley E, et al. Determination of a no-observable effect level for endotoxin following a single intravitreal administration to Dutch Belted rabbits. *Invest Ophthalmol Vis Sci*. 2017;58(3):1545–1552.
5. Bantseev V, Miller PE, Nork TM, et al. Determination of a no observable effect level for endotoxin following a single intravitreal administration to cynomolgus monkeys. *J Ocul Pharmacol Ther*. 2019;35(4):245–253.
6. Jasinska AJ, Lin MK, Service S, et al. A nonhuman primate system for large-scale genetic studies of complex traits. *Hum Mol Genet.* 2012;21(15):3307–3316.
7. Lemere CA, Beierschmitt A, Iglesias M, et al. Alzheimer's disease abeta vaccine reduces central nervous system abeta levels in a non-human primate, the Caribbean vervet. *Am J Pathol.* 2004;165(1):283–297.
8. Cloutier F, Lawrence M, Goody R, et al. Antiangiogenic activity of aganirsen in nonhuman primate and rodent models of retinal neovascular disease after topical administration. *Invest Ophthalmol Vis Sci*. 2012;53(3):1195–203.
9. Glogowski S, Ward KW, Lawrence MS, Goody RJ, Proksch JW. The use of the African green monkey as a preclinical model for ocular pharmacokinetic studies. *J Ocul Pharmacol Ther*. 2012;28(3):290–298.
10. Goody RJ, Hu W, Shafiee A, et al. Optimization of laser-induced choroidal neovascularization in African green monkeys. *Exp Eye Res*. 2011;92(6):464–472.
11. Grishanin R, Vuillemenot B, Sharma P, et al. Preclinical evaluation of ADVM-022, a novel gene therapy approach to treating wet age-related macular degeneration. *Mol Ther*. 2019;27(1):118–129.
12. Hudson N, Celkova L, Hopkins A, et al. Dysregulated claudin-5 cycling in the inner retina causes retinal pigment epithelial cell atrophy. *JCI Insight*. 2019;4(15):e130273.
13. Patel C, Goody R, Hu W, et al. Primate model of chronic retinal neovascularization and vascular leakage. *Exp Eye Res.* 2020;195:108031.
14. Sidman RL, Li J, Lawrence M, et al. The peptidomimetic vasotide targets two retinal VEGF receptors and reduces pathological angiogenesis in murine and nonhuman primate models of retinal disease. *Sci Transl Med*. 2015;7(309):309ra165.
15. Brown Jabs DA, Nussenblatt RB, Rosenbaum JT. Standardization of uveitis nomenclature (SUN) for reporting clinical data. Results of the First International Workshop. *Am J Ophthalmol*. 2005;150:509–516.
16. Hackett RB, McDonald TO. Ophthalmic toxicology and assessing ocular irritation. In: Marzulli FN, Maibach HI, eds. *Dermatotoxicology*. 5th ed. Washington, DC: Hemisphere Publishing; 1996:749–815.
17. Kanski JJ. *Clinical Ophthalmology*. 4th ed. Oxford: Butterworth-Heinemann; 2000;7:263–319.
18. McDonald TO, Shadduck JA. Eye irritation. In: Marzulli FN, Maibach HI, eds. *Advances in Modern Toxicology*. Vol. 4. *Dermatoxicology and Pharmacology*. New York: John Wiley & Sons; 1977:139–191.
19. Munger RJ. Veterinary ophthalmology in laboratory animal studies. *Vet Ophthalmol*. 2002;5:167–175.
20. Nussenblatt RB, Palestine AG, Chan CC, Roberge F. Standardization of vitreal inflammatory activity in intermediate and posterior uveitis. *Ophthalmology*. 1985;92:467–471.
21. Friedman DA, Mason JO, 3rd, Emond T, McGwin G, Jr. Povidone-iodine contact time and lid speculum use during intravitreal injection. *Retina*. 2013;33(5):975–981.
22. Curnow SJ, Murray PI. Inflammatory mediators of uveitis: cytokines and chemokines. *Curr Opin Ophthalmol*. 2006;17(6):532–537.
23. Rageh A, Jordan M, Heuss N, Gregerson D, Ferrington D, Montezuma S. Cytokine production in the endotoxin-induced uveitis model. *Invest Ophthalmol Vis Sci.* 2013;54(15):2049.

24. Satofuka S, Ichihara A, Nagai N, et al. Suppression of ocular inflammation in endotoxin-induced uveitis by inhibiting nonproteolytic activation of prorenin. *Invest Ophthalmol Vis Sci.* 2006;47(6):2686–2692.
25. Shen DF, Chang MA, Matteson DM, Buggage R, Kozhich AT, Chan C. Biphasic ocular inflammatory response to endotoxin-induced uveitis in the mouse. *Arch Ophthalmol.* 2000;118(4):521–527.
26. Deshmane S, Kremlev S, Amini S, Sawaya BE. Monocyte chemoattractant protein-1 (MCP-1): an overview. *J Interferon Cytokine Res*. 2009;29:313–326.